DIRECT CURRENT ELECTRIC POTENTIAL FIELD ASSOCIATED WITH TWO SPHERICAL CONDUCTORS IN A WHOLE-SPACE[1]

D. F. ALDRIDGE and D. W. OLDENBURG[2]

ABSTRACT

ALDRIDGE, D.F. and OLDENBURG, D.W. 1989. Direct current electric potential field associated with two spherical conductors in a whole-space. *Geophysical Prospecting* **37**, 311–330.

Bispherical coordinates are used to derive an exact mathematical solution for the potential field generated by direct current electric conduction in an earth model consisting of two spherical inclusions in a uniform whole-space. The solution takes the form of a spherical harmonic expansion in bispherical coordinates; coefficients in the expansion are obtained by solving sets of linear equations. Rapid forward modelling of numerous interesting situations in d.c. resistivity prospecting is facilitated by the generality and computational efficiency inherent to this new solution. For example, the accuracy of image (or superposition) methods for calculating potential solutions can be quantified. Similarly, the ability of d.c. conduction methods to resolve two distinct bounded bodies in three-dimensional space can be examined by repeatedly calculating the secondary potential or apparent resistivity response of an earth model as a selected parameter is varied. Synthetic mise à la masse, crosshole, or areal potential data sets can be generated for subsequent use in inversion studies. Improvements in solution technique derived here also apply to a simpler model consisting of a single sphere buried in a half-space.

INTRODUCTION

Classical electric potential solutions are useful in geophysical prospecting for several reasons. They provide a means for making order of magnitude estimates of the influence of various geometrical and material parameters on the size, shape, extent and polarity of a measured anomaly. With a closed form mathematical solution, such tests can be conducted rapidly, accurately and cheaply. Furthermore, they can

311

serve as analytical controls for programs that calculate potential solutions by numerical techniques. This is of particular importance for monitoring the accuracy and stability of a computational algorithm. Finally, they are valuable as educational tools.

In this paper we extend the limited repertoire of classical potential solutions to include a model consisting of two spherical bodies of finite conductivity embedded within a uniform whole-space. With this solution, we are able to address an important and practical question concerning d.c. resistivity prospecting methods: what is the resolving power of the technique? Or, in terms of our assumed earth model, under what conditions (such as separation, sizes, resistivity contrast, electrode geometry) can the presence of two separate and distinct mineral bodies be inferred from a measured potential anomaly? Unlike prospecting methods based on wave propagation, where the wavelength of the incident radiation provides an intrinsic length scale with which to quantify resolving power, the resolution capabilities of static (i.e. zero frequency) potential methods can only be assessed via modelling studies. With an analytical solution to a full 3D problem, these studies can be conducted at a fraction of the cost associated with numerical techniques. Questions concerning the accuracy of the analytical approach still arise, but they are usually of minor importance compared with the theoretical and computational approximations inherent to most numerical modelling schemes.

Figure 1 depicts the earth model used in this investigation and defines the coordinate frame of reference. All three media are considered electrically linear, homogeneous and isotropic. A point source of d.c. electric current is located at S with coordinates (x_s, y_s, z_s) and emits conventional current I. The problem is to calculate the potential (relative to infinity) at the field point P with coordinates (x, y, z). Once this solution is obtained, the potential difference measured by a more complicated voltage/current electrode arrangement can be constructed by superposition principles.

The electric potential satisfies Laplace's equation $\nabla^2 V = 0$ everywhere except at S. A bispherical coordinate description is adopted because: (1) Laplace's equation is separable in these coordinates (after factoring out a modulating function – see (8)), and (2) the physical surfaces of the assumed earth model are coincident with level surfaces of this coordinate frame. Appendix A gives the transformations between rectangular coordinates (x, y, z) and bispherical coordinates (μ, η, ϕ).

Several investigators have used bispherical coordinates to study the potential field associated with a single spherical body buried in a half-space and subject to d.c. current flow from a nearby point electrode (Lipskaya 1949; Van Nostrand 1953; Large 1971; Merkel and Alexander 1971; Snyder and Merkel 1973). The mathematical technique we employ to analyse the 'two spheres in a whole-space' problem is a straightforward extension of that described by Large (1971). However, our reformulation of the mathematics yields a set of equations that possesses significant computational advantages over those previously published. The improvement manifests itself practically when modelling potential surveys where the position of the current source changes frequently. Basically, the set of matrices that needs to be inverted to obtain the potential solution can be made *independent* of the current source coordi-
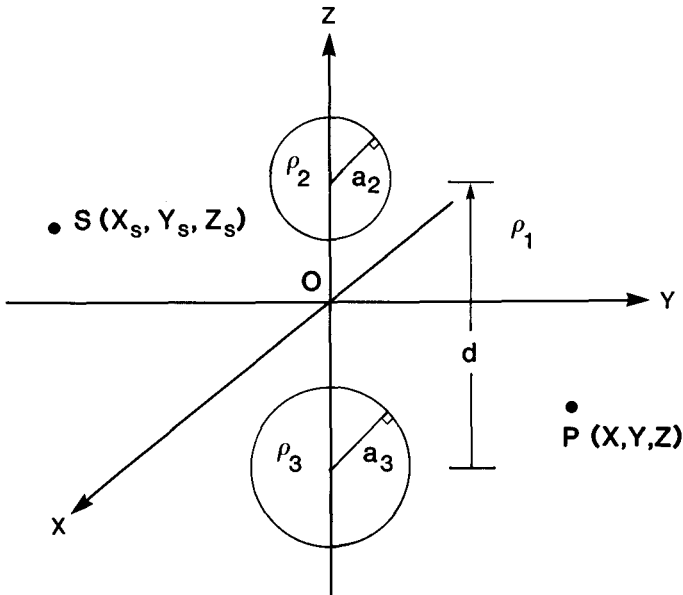
FIG. 1. Earth model and rectangular coordinate reference system. a_2, a_3 are the sphere radii; ρ_2, ρ_3 the sphere resistivities; d the sphere centre separation; and ρ_1 the whole-space resistivity. Source point S and field point P may be located anywhere (including within the spheres).

nates (μ_s, η_s, ϕ_s). Hence, only one set of matrix inversions per earth model needs to be performed.

The following sections give the mathematical derivation for the more complicated two-sphere situation in detail. It is evident that the improvement in the solution technique can also be applied to the simpler one-sphere problem. We merely state the relevant equations for this case, leaving the derivation for the interested reader. The final equations for potential given here (for both earth models) are completely general; the current electrode position (μ_s, η_s, ϕ_s) and the field point position (μ, η, ϕ) are not artificially restricted in any way. Previous studies have incorporated various limitations into the final results: the source location has been restricted to the surface of the half-space ($\mu_s = 0$), the x axis ($\phi_s = 0$), or directly over the buried sphere centre ($\eta_s = \pi$); the voltage receiver position has often been limited to the half-space surface also. Obviously, more general equations are necessary to model surface-to-surface, surface-to-borehole, borehole-to-surface and borehole-to-borehole potential surveys. Our results offer an improvement in this respect.

THEORETICAL DEVELOPMENT

The potentials in the unbounded medium and within the two spherical bodies are designated V_1, V_2 (for $z > 0$), and V_3 (for $z < 0$), respectively. We adopt the usual

procedure of separating each potential into a reference (or primary) potential and a perturbation (or secondary) potential. An appropriate reference potential for our problem is that due to a point source of d.c. electric current located in a homogeneous and isotropic whole-space. Hence

$$V_1 = V_w + V_{1s}, \tag{1}$$

$$V_2 = V_w + V_{2s}, \tag{2}$$

$$V_3 = V_w + V_{3s}, \tag{3}$$

where the wholespace potential V_w is given by

$$V_w = \frac{\rho_s I}{4\pi R}. \tag{4}$$

ρ_s is the resistivity of the material at the source position and R is the distance between source and observation points.

The secondary potentials of (1)–(3) are perturbations on a background potential due to the presence of the two spherical bodies. Since the whole-space potential is a solution of Laplace's equation, application of the Laplacian operator to (1)–(3) demonstrates that these secondary potentials also satisfy Laplace's equation. Hence, each may be represented as spherical hermonic expansion in bispherical coordinates (Grant and West 1965, p. 423; Wyld 1976, chapter 3):

$$V_{1s}(\mu, \eta, \phi) = F \sum_{l=0}^{\infty} \sum_{m=-l}^{+l} [A_{lm} e^{-(l+1/2)\mu} + B_{lm} e^{+(l+1/2)\mu}] Y_l^m(\eta, \phi), \tag{5}$$

$$V_{2s}(\mu, \eta, \phi) = F \sum_{l=0}^{\infty} \sum_{m=-l}^{+l} C_{lm} e^{-(l+1/2)\mu} Y_l^m(\eta, \phi), \tag{6}$$

$$V_{3s}(\mu, \eta, \phi) = F \sum_{l=0}^{\infty} \sum_{m=-l}^{+l} D_{lm} e^{+(l+1/2)\mu} Y_l^m(\eta, \phi). \tag{7}$$

$Y_l^m(\eta, \phi)$ is the spherical harmonic of degree l and order m. The spherical harmonics constitute an orthonormal set of basis functions for expansion of an arbitrary function in 2D angular coordinates. The precise definition of the spherical harmonics is stated in Appendix B along with some of their properties that are used in the sequel. Note that a single exponential term of appropriate sign is included in (6) and (7) in order that the potentials remain bounded as μ approaches $\pm \infty$. Finally, F is a multiplicative factor with dimensions of electric potential that occurs repeatedly in the formulae. It depends on both source and field point coordinates and is given by

$$F = \left(\frac{\rho(\mu_s, \eta_s, \phi_s) I}{4\pi b} \right) \sqrt{\cosh \mu_s - \cos \eta_s} \, \sqrt{\cosh \mu - \cos \eta}. \tag{8}$$

The bispherical coordinate system scale factor b is determined by the sphere radii a_2 and a_3 and centre separation d, and is given in Appendix A.

An immediate reduction in the number of unknown coefficients in the above equations is effected by requiring the total potential to be continuous at the two

spherical interfaces μ_2 and μ_3:

$$V_1(\mu_2, \eta, \phi) = V_2(\mu_2, \eta, \phi),$$ (9a)

$$V_1(\mu_3, \eta, \phi) = V_3(\mu_3, \eta, \phi).$$ (9b)

Application of these boundary conditions yields

$$C_{lm} = A_{lm} + B_{lm} e^{+(2l+1)\mu_2},$$ (10a)

$$D_{lm} = A_{lm} e^{-(2l+1)\mu_3} + B_{lm}.$$ (10b)

The remaining unknown coefficients A_{lm} and B_{lm} are determined by applying the boundary condition regarding the continuity of normal current flow at the spherical interfaces. Once all coefficients are known, (5)–(7) provide a mechanism for calculating the secondary potentials. The spherical harmonic expansions are simply evaluated up to the maximum degree l consistent with series convergence and the finite precision of a digital computer. The calculation is valid at all locations (x, y, z) including the source position (x_s, y_s, z_s); the singular behaviour associated with the current source is contained entirely within the whole-space potential term.

The final boundary conditions are mathematically expressed as

$$\frac{1}{\rho_1} \frac{\partial V_1}{\partial \mu}\bigg|_{\mu_2} = \frac{1}{\rho_2} \frac{\partial V_2}{\partial \mu}\bigg|_{\mu_2},$$ (11a)

$$\frac{1}{\rho_1} \frac{\partial V_1}{\partial \mu}\bigg|_{\mu_3} = \frac{1}{\rho_3} \frac{\partial V_3}{\partial \mu}\bigg|_{\mu_3}.$$ (11b)

Utilizing (1)–(3) these become

$$\frac{\rho_1}{\rho_2} \frac{\partial V_{2s}}{\partial \mu}\bigg|_{\mu_2} - \frac{\partial V_{1s}}{\partial \mu}\bigg|_{\mu_2} = \left(1 - \frac{\rho_1}{\rho_2}\right) \frac{\partial V_w}{\partial \mu}\bigg|_{\mu_2},$$ (12a)

$$\frac{\rho_1}{\rho_3} \frac{\partial V_{3s}}{\partial \mu}\bigg|_{\mu_3} - \frac{\partial V_{1s}}{\partial \mu}\bigg|_{\mu_3} = \left(1 - \frac{\rho_1}{\rho_3}\right) \frac{\partial V_w}{\partial \mu}\bigg|_{\mu_3}.$$ (12b)

Evaluation of the left-hand sides of these equations requires expressions for the derivatives of the secondary potentials V_{1s}, V_{2s} and V_{3s}. These are obtained via straightforward, but tedious, differentiation of the expansions (5), (6) and (7). To evaluate the right-hand sides of the boundary condition equations, we require a spherical harmonic expansion of the whole-space potential. Equation (4) is transformed to bispherical coordinates by substitution from (A4)–(A6):

$$V_w = \left(\frac{\rho(x_s, y_s, z_s)I}{4\pi}\right)[(x - x_s)^2 + (y - y_s)^2 + (z - z_s)^2]^{-1/2}$$

$$= F\{2[\cosh(\mu - \mu_s) - \cos \Theta]\}^{-1/2},$$ (13)

where the angle Θ satisfies

$$\cos \Theta = \cos \eta \cos \eta_s + \sin \eta \sin \eta_s \cos(\phi - \phi_s).$$ (14)

The reciprocal square root term in (13) is now expanded as an infinite series in Legendre polynomials with argument $\cos \Theta$. The 'generating function' theorem for

Legendre polynomials (B7) is used. Next, the spherical harmonic addition theorem ((B4) and (B5)) is used to rewrite the Legendre polynomials in terms of spherical harmonics in source and field point coordinates. The result is

$$V_w(\mu, \eta, \phi) = F \sum_{l=0}^{\infty} \sum_{m=-l}^{+l} \left(\frac{4\pi}{2l+1}\right) e^{-(l+1/2)|\mu - \mu_s|} Y_l^m(\eta_s, \phi_s)^* Y_l^m(\eta, \phi). \tag{15}$$

This expression can be differentiated and the result substituted into the boundary condition equations. One must be careful to use the proper 'form' of (15) depending on whether the source is located in the upper sphere ($\mu_s > \mu_2 > \mu_3$), in the unbounded medium ($\mu_2 > \mu_s > \mu_3$), or within the lower sphere ($\mu_2 > \mu_3 > \mu_s$). All of these situations are of interest in modelling studies.

The procedure described by Large (1971) is now used to reduce the boundary conditions (12a) and (12b) to a system of linear equations in the unknown coefficients A_{lm} and B_{lm}. After substitution of the expressions for the derivatives of the potentials and cancelling common factors, multiply by $Y_k^n(\eta, \phi)^* \sin \eta$ and integrate over the full range of η and ϕ. We exploit the orthonormality property of the spherical harmonics (B2) and the additional 'sum and integral' property given by (B6). Persisting through a major amount of algebraic reduction transforms (12a) and (12b) to

$$\left(\frac{\rho_1}{\rho_2} - 1\right)[\alpha_{l-1,m}(\mu_2)A_{l-1,m} + \beta_l(\mu_2, 1)A_{lm} + \gamma_{l+1,m}(\mu_2)A_{l+1,m}]$$

$$+ \left(\frac{\rho_1}{\rho_2} + 1\right)[\alpha_{l-1,m}(-\mu_2)B_{l-1,m} + \beta_l(-\mu_2, \chi_{12})B_{lm} + \gamma_{l+1,m}(-\mu_2)B_{l+1,m}]$$

$$= 2\pi\left(1 - \frac{\rho_1}{\rho_2}\right)\delta_{lm}(\mu_2, -\mu_s; \eta_s, \phi_s), \tag{16a}$$

$$\left(\frac{\rho_1}{\rho_3} + 1\right)[\alpha_{l-1,m}(\mu_3)A_{l-1,m} + \beta_l(\mu_3, \chi_{13})A_{lm} + \gamma_{l+1,m}(\mu_3)A_{l+1,m}]$$

$$+ \left(\frac{\rho_1}{\rho_3} - 1\right)[\alpha_{l-1,m}(-\mu_3)B_{l-1,m} + \beta_l(-\mu_3, 1)B_{lm} + \gamma_{l+1,m}(-\mu_3)B_{l+1,m}]$$

$$= 2\pi\left(1 - \frac{\rho_1}{\rho_3}\right)\delta_{lm}(-\mu_3, \mu_s; \eta_s, \phi_s). \tag{16b}$$

Functions appearing in these equations are defined in Appendix C. Equations (16a) and (16b) are appropriate for a current source located in the unbounded medium of resistivity ρ_1. If the source is placed within one of the spherical bodies, the right-hand side of one equation is altered slightly; the correct forms are also given in Appendix C.

SYSTEMS OF LINEAR EQUATIONS

Despite the formidable appearance of (16a) and (16b), they are structurally simple and similar. Suppose that the maximum degree spherical harmonic included in the solution for the secondary potentials is $l = l_{max}$. Then, for fixed order m, (16a) and

(16b) together represent a system of $2 (l_{max} + 1 - |m|)$ linear equations in the unknown constants A_{lm} and B_{lm}. They are solved via standard techniques of linear algebra. However, we do not need to solve linear equations to obtain the expansion coefficients for negative orders. Analysis indicates that the constants A_{lm} and B_{lm} possess the same Hermitian symmetry/skew-symmetry as the spherical harmonics (B3):

$$A_{l, -m} = (-1)^m A_{lm}^*, \qquad B_{l, -m} = (-1)^m B_{lm}^*.$$

Substitution of these relations into (5) yields

$$V_{1s}(\mu, \eta, \phi) = F \sum_{l=0}^{\infty} \sum_{m=0}^{+l} d_m [e^{-(l+1/2)\mu} \mathscr{R}\{A_{lm} Y_l^m(\eta, \phi)\}$$

$$+ e^{+(l+1/2)\mu} \mathscr{R}\{B_{lm} Y_l^m(\eta, \phi)\}], \tag{17}$$

where $d_m = 2 - \delta_{0m}$ and $\mathscr{R}\{ \ \}$ indicates real part of $\{ \ \}$. Similar results are easily derived for the secondary potentials V_{2s} and V_{3s}.

The linear system of equations (16a) and (16b) is compactly represented in matrix notation as

$$\mathbf{C}_m \mathbf{x}_m = \mathbf{b}_m, \qquad (m = 0, 1, 2, \cdots l_{max}) \tag{18}$$

where $\mathbf{x}_m$ is a vector of unknowns given by $\{A_{mm}, \ldots, A_{l_{max}, m}, B_{mm}, \ldots, B_{l_{max}, m}\}$. Dependence upon source and earth model parameters is given by

$$\mathbf{C}_m = \mathbf{C}_m\left(\mu_2, \mu_3, \frac{\rho_1}{\rho_2}, \frac{\rho_1}{\rho_3}\right), \tag{19}$$

$$\mathbf{b}_m = \mathbf{b}_m\left(\mu_2, \mu_3, \frac{\rho_1}{\rho_2}, \frac{\rho_1}{\rho_3}; \mu_s, \eta_s, \phi_s\right). \tag{20}$$

Here we note the major benefit that accrues from the current formulation of the problem. The matrix $\mathbf{C}_m$ depends *only* upon the assumed earth model (ρ_1, ρ_2, ρ_3, a_2, a_3, d). Source position dependence is contained entirely within the right-hand side column vector $\mathbf{b}_m$. Hence, the set of matrices $\mathbf{C}_m$ needs to be generated and inverted only once per earth model. Each time the current source is relocated, only the vector $\mathbf{b}_m$ is altered. Calculation of each new set of spherical harmonic expansion coefficients A_{lm} and B_{lm} reduces to a set of trivial matrix-vector multiplications. This provides an obvious computational advantage when modelling profiling, sounding, areal or borehole resistivity surveys where the current electrodes change position often. Large's (1971) equations do not exhibit this characteristic, although they could probably be put into this form.

Several special cases serve as useful checks on the lengthy algebra of the derivation. Hence, if $\rho_1 = \rho_2 \neq \rho_3$, then (16a) and (16b) indicate that the B_{lm} elements of the solution vector are zero. Thus, $V_{2s} = V_{1s}$, as expected. Similarly, if $\rho_1 = \rho_3 \neq \rho_2$, then $A_{lm} = 0$ and $V_{3s} = V_{1s}$. The trivial solution $\mathbf{x}_m = 0$ is generated by $\rho_1 = \rho_2 = \rho_3$; all secondary potentials reduce to zero and $V_1 = V_2 = V_3 = V_w$. Finally, the case of a current source located on the axis of symmetry $x = y = 0$ is examined. In this situation $\cos \eta_s = \pm 1$ and the spherical harmonics evaluated at the source coordi-

nates are equal to zero for all orders m not equal to zero. Equation (C4), together with the previous equations, indicates that the solution vector $\mathbf{x}_m = 0$ for all orders $m \neq 0$. Only the zero-order spherical harmonic enters into the solution for the secondary potentials. But, as indicated in Appendix A, the zero-order spherical harmonics are independent of the azimuthal angle ϕ. This axial symmetry in the calculated potentials is entirely appropriate for the assumed location of the current source and arises quite naturally from the system of equations derived here. One need not appeal to a 'degeneracy' in the system to obtain this result (Large 1971).

SINGLE SPHERE IN A HALF-SPACE

A limiting case of this general potential solution is valid for an earth model consisting of a single spherical inclusion within a uniform half-space. In terms of Fig. 1, the sphere centre is located on the positive z axis and the half-space $z < 0$ is considered to be a vacuum. The appropriate expressions are obtained by passing to the limit as $a_3 \to \infty$, $d - a_3 \to h$ where h is the centre depth of the buried sphere, and $\rho_3 \to \infty$. The procedural details are omitted here. If V_{1s} and V_{2s} are the secondary potentials exterior to and interior to the buried sphere, and V_{3s} is the secondary potential within the insulating half-space, then we obtain

$$V_{1s}(\mu, \eta, \phi) = 2F \sum_{l=0}^{\infty} \sum_{m=0}^{l} d_m \cosh\left[(l + \tfrac{1}{2})\mu\right] \mathscr{R}\{B_{lm} Y_l^m(\eta, \phi)\}, \tag{21}$$

$$V_{2s}(\mu, \eta, \phi) = 2F \sum_{l=0}^{\infty} \sum_{m=0}^{l} d_m \cosh\left[(l + \tfrac{1}{2})\mu_2\right] e^{-(l+1/2)(\mu - \mu_2)} \mathscr{R}\{B_{lm} Y_l^m(\eta, \phi)\}, \tag{22}$$

$$V_{3s}(\mu, \eta, \phi) = 2F \sum_{l=0}^{\infty} \sum_{m=0}^{l} d_m\, e^{+(l+1/2)\mu} \mathscr{R}\{B_{lm} Y_l^m(\eta, \phi)\} + \frac{\rho_s I}{4\pi}\left[\frac{1}{R} - \frac{1}{R'}\right]. \tag{23}$$

The expression for the scalar b (in the factor F) obtained by taking the limit of (A9) agrees with that given by Large (1971). These perturbation potentials are specified relative to a half-space reference potential given by

$$V_h = \frac{\rho_s I}{4\pi}\left[\frac{1}{R} + \frac{1}{R'}\right]. \tag{24}$$

R is the usual source to receiver distance and R' is the distance from the image source position to the field point P.

The expansion coefficients B_{lm} satisfy the following set of linear equations:

$$a_{l-1,m} B_{l-1,m} + b_l B_{lm} + c_{l+1,m} B_{l+1,m} = d_{lm}. \tag{25}$$

Quantities a_{lm}, b_l, c_{lm} and d_{lm} are defined in Appendix C. This system of equations also has the favourable property that dependence on the source coordinates (μ_s, η_s, ϕ_s) is contained solely within the right-hand side quantities d_{lm}.

Our first use of these equations for modelling purposes is displayed in Fig. 2. Each frame depicts the secondary potential measured along a line on the surface of
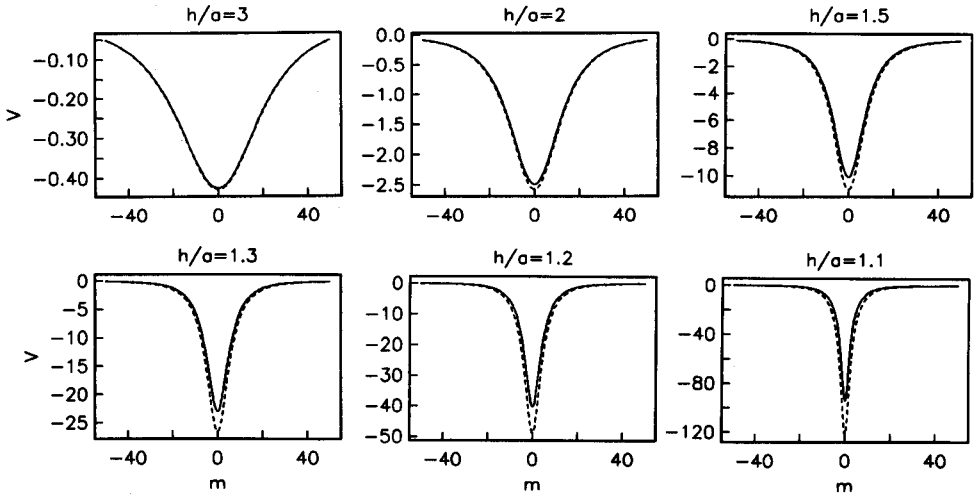
FIG. 2. Comparison of exact (——) and image (– – –) methods for calculating secondary potential on the surface of a half-space containing a buried sphere. h is centre depth and a is radius of sphere. $\rho_1 = 1000\ \Omega\text{m}$; $\rho_1/\rho_2 = 100$; $a = 10$ m. Current source is located directly over sphere centre at $x = 0$ and emits 1 A.

a half-space directly over a buried spherical conductor. Successive frames are labelled with the centre depth-to-radius ratio for the sphere. The solid curves are exact calculations of the potential anomaly via (21) and (25); the dashed curves are approximate calculations using an elementary image method. The image solution technique involves superposing two 'sphere in a whole-space' solutions in their correct geometrical relation. Where the current source and voltage receiver are both located on the half-space surface, this superposition amounts to multiplying the whole-space calculation by four (one factor of two accounts for the difference in earth models and the other factor of two accounts for the different reference potentials adopted). The image method of solution is useful because it is much easier to implement than the exact calculation.

Although there is nothing particularly novel about either type of curve, they do allow us to make a quantitative evaluation of the accuracy of the image solution technique. A frequently stated rule of thumb is that the image technique yields an accurate solution if the ratio of centre depth-to-radius exceeds 1.3 (Grant and West 1965, p. 425; Telford et al. 1976, p. 649). Furthermore, this rule is often taken to apply in an approximate sense to various non-spherical bodies of geological interest. Since the absolute value of the potential anomaly increases dramatically as the sphere becomes shallower, we show the percentage difference between the two curves in Fig. 3a. An alternative representation of the error in terms of apparent resistivity ($\rho_a = 2\pi R V_1 / I$ where V_1 is total potential) is depicted in Fig. 3b. These plots indicate that the accuracy of the image method of solution is influenced by the depth-to-radius ratio h/a and the measurement position x. Similar modelling with a sphere with reduced resistivity contrast demonstrates that the overall level of the
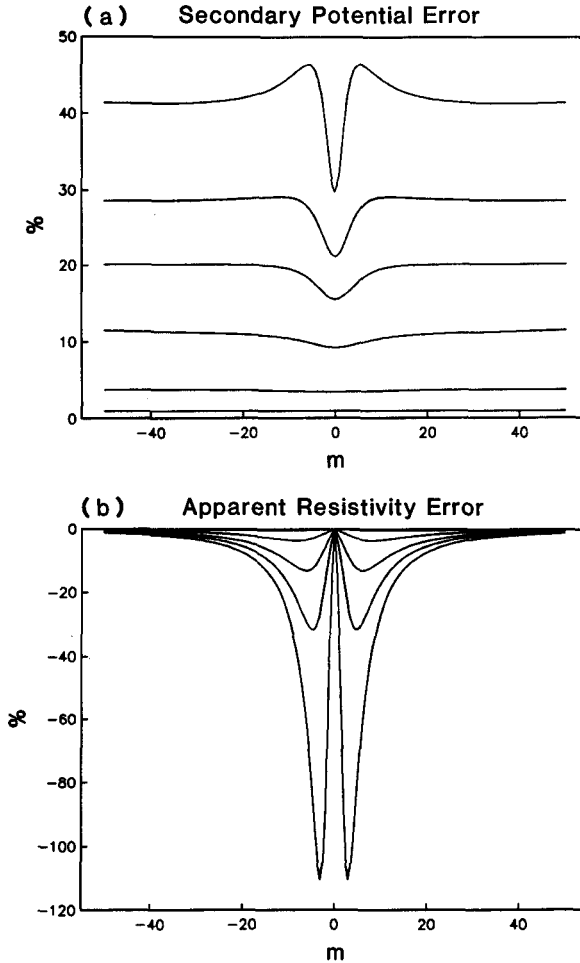
FIG. 3. (a) Percentage difference between the secondary potential curves of Fig. 2. Plotted curves are $p = 100(V^a/V^e - 1)$ where V^a and V^e are approximate and exact calculations. From top to bottom, curves are for $h/a = 1.1, 1.2, 1.3, 1.5, 2, 3$. (b) Percentage difference between apparent resistivity curves implied by the approximate and exact secondary potentials of Fig. 2. Plotted curves are $p = 100(\rho^a/\rho^e - 1)$ where ρ^a and ρ^e are approximate and exact calculations. From top to bottom curves are for $h/a = 3, 2, 1.5, 1.3, 1.2, 1.1$. First two curves plot virtually on top of 0% axis.

error curves is depressed; hence the resistivity ratio ρ_1/ρ_2 also has an effect. We can easily see that these error curves will be altered in detail if the current source is relocated or a more complicated electrode geometry is employed. Again, modelling can provide a quantitative assessment of the relative error.

An analogous procedure is used to quantify the effect of electrical interaction between two spherical conductors embedded in a whole-space. We are interested in
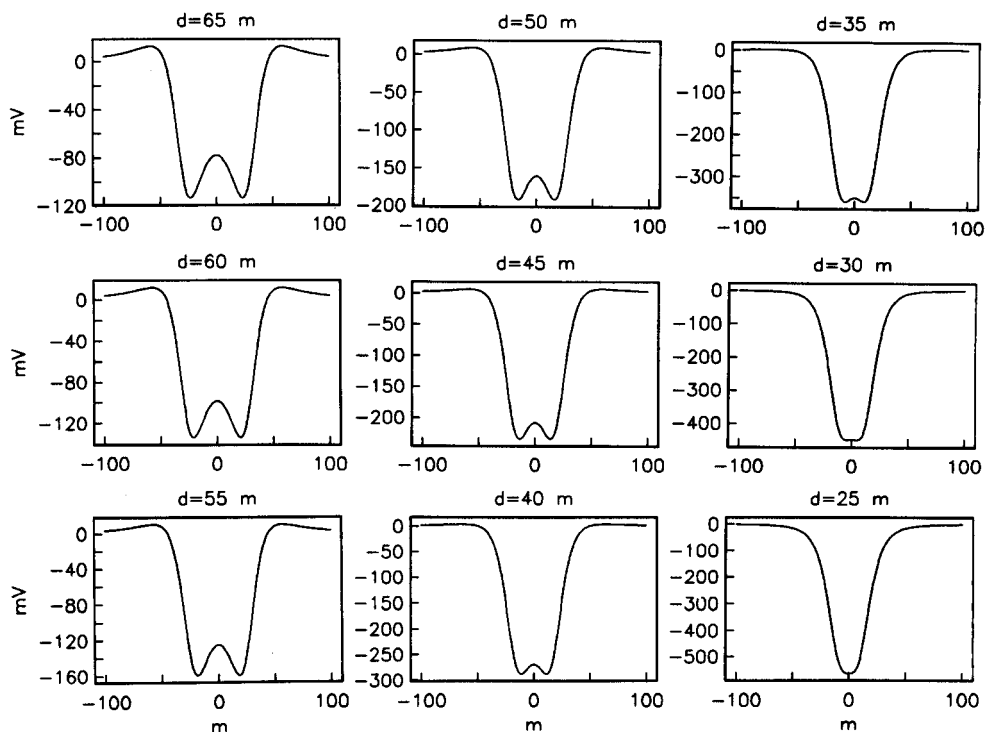
FIG. 4. Resolution study for two spheres of equal radii ($a_2 = a_3 = 10$ m) and equal resistivities ($\rho_2 = \rho_3 = 10$ Ωm) embedded within a whole-space ($\rho_1 = 1000$ Ωm). Line of voltage receivers is offset $h = 20$ m from the z-axis. Current source (emitting 1 A) is fixed at centre of recording line.

those conditions whereby simple superposition of two 'sphere in a whole-space' solutions yields an inaccurate result at a specified tolerance level. For the special case of two spherical bodies of equal radii and equal resistivities, the error curves of Fig. 3 are reproduced exactly (assuming, of course, identical parameter values and electrode geometry). The curves are merely relabelled with the ratio of centre separation to twice the common radius $d/2a$.

RESOLVING TWO SPHERES

Resolution refers to the ability of an experimental or interpretational procedure to distinguish the presence of separate entities in a measured composite response. The ability of d.c. electrical conduction methods to resolve two distinct ore bodies can be examined via modelling experiments based on the above equations for secondary potentials. We do not attempt to derive general theoretical conditions under which two buried spherical bodies may or may not be resolved; there are too many variables (sphere radii, resistivities and separation; electrode geometry). Rather, we
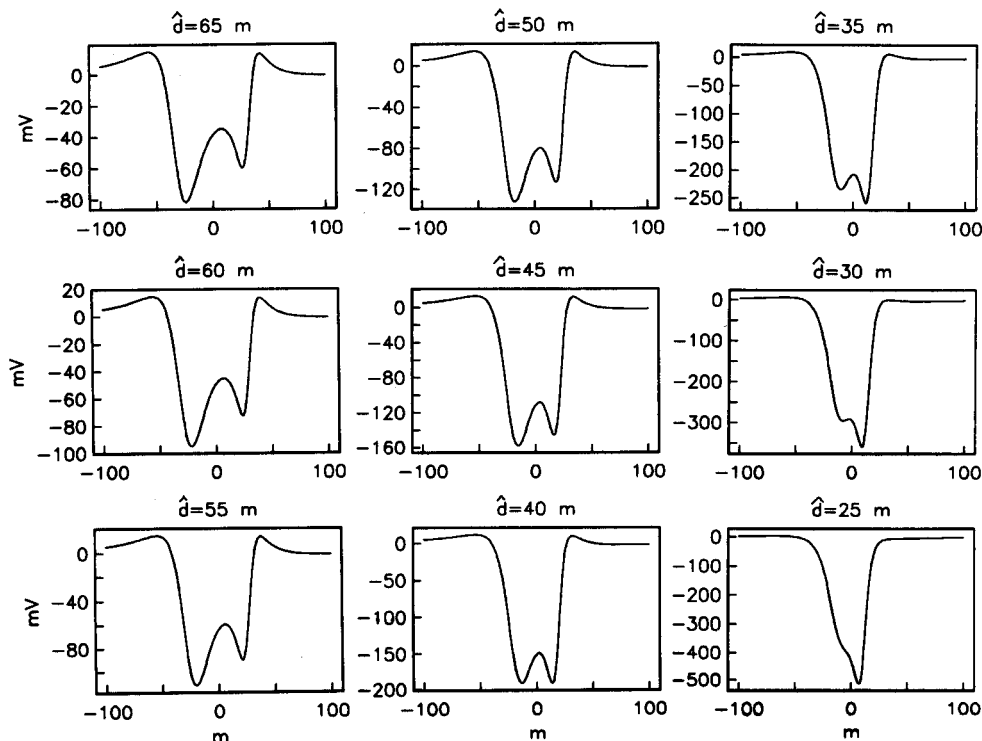
FIG. 5. Resolution study for two spheres of unequal radii ($a_2 = 5$ m, $a_3 = 10$ m) and unequal resistivities ($\rho_2 = 10$ Ωm, $\rho_3 = 75$ Ωm) embedded within a whole-space ($\rho_1 = 1000$ Ωm). For each frame, the line of voltage receivers is reoriented to maintain $h_2/a_2 = h_3/a_3 = 2$. h_2 and h_3 are perpendicular distances from voltage recording line to sphere centres within $z > 0$ and $z < 0$, respectively. Frames are labelled with the distance between sphere centres projected on to this recording line. Current source (emitting 1 A) is maintained at centre of recording line.

formulate a modelling technique whereby the resolvability of two spherical bodies can be quantitatively evaluated for specified, but nevertheless arbitrary, earth model parameters and source/receiver configurations.

Figures 4 and 5 present the results of resolution studies for the two-sphere problem. A single fixed current electrode (emitting 1 A) is used. The potential anomaly measured along a line of voltage receivers extending 100 m on either side of the source is plotted. These secondary potentials simulate what would be detected in a deep borehole in the vicinity of the two spheres when all other perturbing influences (including the surface) are far away. Alternatively, if we rotate our per-spective by 90° and scale the potentials by a factor of four, they approximate the anomalies that would be detected on the surface of a halfspace due to a surface current source. Although we cannot solve exactly for the potential field associated with the 'two spheres in a half-space' model, Figs 2 and 3 suggest that the image method of solution will yield a reasonably accurate result if the depth-to-radius

ratio for the spheres exceeds two. We adhere to this criterion in all of the following resolution studies. Since the absolute value of the potential anomaly increases significantly as separation distance decreases, a different voltage scale is assigned to each frame of the figures. The shape of the curves is thus emphasized at the expense of the overall amplitude of the anomaly.

Figure 4 depicts the voltage anomaly as centre separation changes for a symmetrical situation consisting of two spheres of equal radii and equal resistivities. If peaks or troughs in the composite response are used to infer the presence of separate buried bodies, then the resolution limit for this case occurs somewhere between 30 m and 25 m separation distance. Note that a borehole drilled on the central portion of the anomaly would not encounter the target; even at 25 m centre separation, there still exists a 5 m gap between the sphere boundaries. The theoretical limit of resolution corresponds to a separation where the centre of the potential anomaly exhibits zero curvature or a "flat spot" (Elkins and Hammer 1938). This is precisely the same as the so-called Ricker resolution limit (Ricker 1953; Kallweit and Wood 1982) for thin bed detection in seismic reflection prospecting. In principle, analysis of the shape and amplitude of the anomaly could resolve bodies separated by less than this Ricker limit. In practice, the ability to accomplish this will be inhibited by noise contamination and amplitude calibration problems for the small secondary potentials involved.

A resolution study for a completely asymmetrical model consisting of two spherical bodies of unequal radii and unequal resistivities is shown in Fig. 5. We attempt to equalize the amplitude of the anomaly produced by each body by equating: (1) the product of sphere volume and relative conductivity $4/3\pi a^3$ $(\sigma - \sigma_1)$, and (2) the centre depth-to-radius ratio h/a, for each of the two spheres. As the centre separation distance is reduced, the line of voltage receivers must be reoriented in the xyz coordinate system to maintain this second condition. Hence, when viewed from this recording line, the earth model appears to be two spheres of different sizes at different (but fixed) depths. Each frame is labelled with the distance between the sphere centres projected on to this line. The smaller sphere produces a sharper kick on the composite voltage anomaly curve than the larger sphere; each curve also possesses a distinct asymmetry. However, at the smaller separation distances, it is doubtful that this asymmetry would be recognized, and its significance correctly ascertained, in a real prospectng context. The practical limit of resolution for this earth model probably also lies somewhere between 30 m and 25 m separation. This still leaves a 10 m gap between sphere boundaries (projected on to the recording line).

We have re-executed the above two resolution studies where the line of voltage receivers is positioned nearer $(h/a = 1.5)$ and farther $(h/a = 3)$ from the sphere centres. In each case a different resolution limit is inferred from the voltage anomaly curves. Obviously, the location of the electrodes relative to the assumed earth model plays a basic role in resolvability. Furthermore, our electrode configuration is deliberately chosen to be simple in order to illustrate the resolution phenomenon. Here we do not address the important issue of which current source and voltage receiver geometry possesses the highest resolving power, for a given earth model. However, such a study could be conducted utilizing the potential solution derived above.

Our final examples illustrate the effect of altering the current electrode position within a fixed earth model. Mise à la masse methods are often used to assess the spatial extent of a buried mineral deposit. Any lack of lateral continuity in the deposit should have an expression in terms of the measured potential anomaly at the surface. However, these gaps in mineralization may be unresolved by the measurement geometry. Figure 6 displays the mise à la masse response of two spherical conductors separated by a narrow 5 m gap. A point current electrode is located within one of the spheres 2 m below its upper boundary. The voltage recording
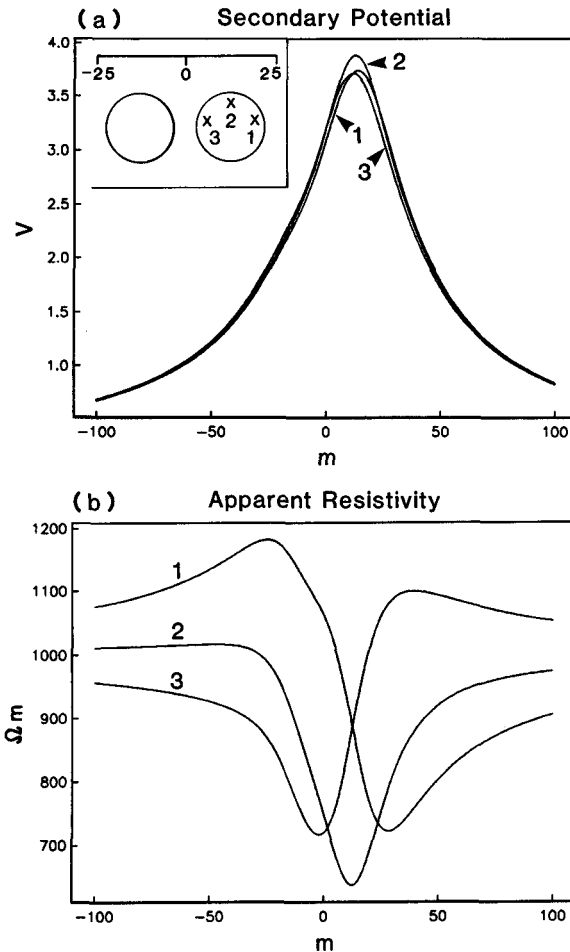

FIG. 6. Mise à la masse modelling for two buried spherical bodies. (a) Secondary potentials. (b) Apparent resistivities. $a_2 = a_3 = 10$ m; $d = 25$ m; $\rho_2 = \rho_3 = 50$ Ωm; $\rho_1 = 1000$ Ωm. Line of voltage receivers is offset $h = 20$ m from z-axis. Each curve refers to a specific current source location within the buried sphere in the half-space $z > 0$. Curves 1–3 are for $z_s = 20.5$, 12.5, 4.5 m; $x_s = 4$, 8, 4 m; $y_s = 0$, respectively.
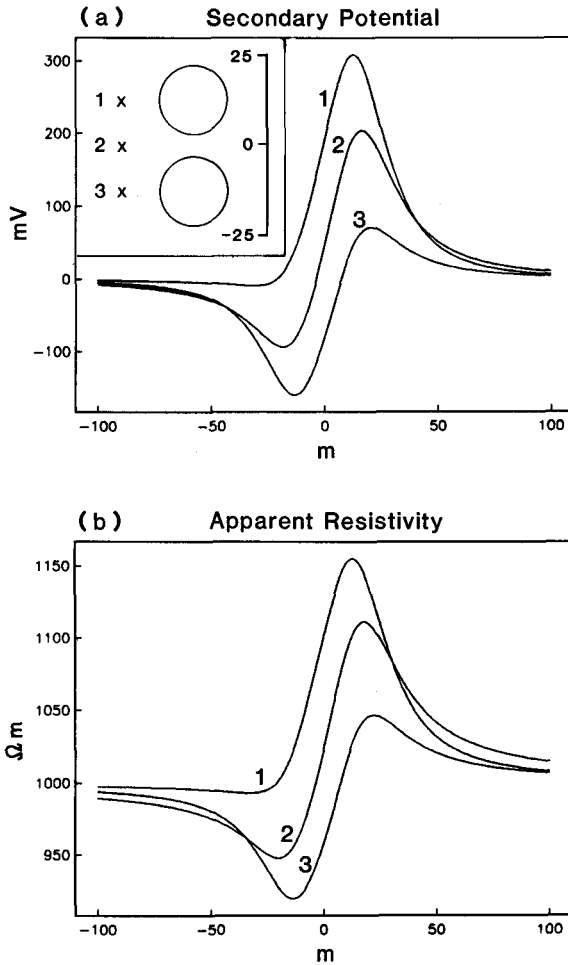
FIG. 7. Synthetic crosshole potential data. (a) Secondary potentials. (b) Apparent resistivities. $a_2 = a_3 = 10$ m; $d = 25$ m; $\rho_2 = 100$ Ωm; $\rho_3 = 10\,000$ Ωm; $\rho_1 = 1000$ Ωm. Source and receiver holes are offset $h = 20$ m from z-axis. Curves 1–3 refer to $z_s = 12.5$, 0, -12.5 m, respectively.

spread is fixed to the ground and centred over the gap. Repositioning the source within the sphere produces only minor changes in the secondary potential curves. The apparent resistivity curves ($\rho_a = 4\pi R V_1/I$ where V_1 is total potential) show a much greater sensitivity to the current source location, but are not unambiguously interpreted in terms of a resistive zone cutting through a conductive ore deposit. Finally, Fig. 7 displays a synthetic crosshole potential data set. Two spherical bodies of equal radii are again separated by a 5 m gap and are located between the source and receiver holes. The secondary potential and apparent resistivity responses are

strongly influenced by the current electrode location. A naive interpretation of the apparent resistivity values would mislocate both the resistive and conductive bodies between the holes.

CONCLUSION

A theoretical solution for the electric potential field associated with two spherical conductors embedded within a uniform whole-space has been given. The form of the solution is a spherical harmonic expansion in bispherical coordinates; coefficients in the expansion are obtained by solving sets of linear equations. Although the analytical technique used for solution is an extension of a previously known method, an improved structure of the governing equations that allows for enhanced computational efficiency has been demonstrated. This feature is of particular importance for generating large-scale synthetic data sets for use in inversion studies. The improvement in solution technique applies equally well to a simpler earth model consisting of a single spherical body in a half-space. When implemented on a digital computer, the potential solution is not exact in a mathematical sense because the spherical harmonic expansions must be truncated at a finite number of terms. Numerical testing indicates that ten terms (in the degree l) is usually more than adequate to obtain series convergence with a relative precision of 0.5%.

The final equations for potential (for each earth model) are of sufficient generality to enable modelling of numerous interesting situations in d.c. resistivity prospecting involving bounded bodies in 3D space. Two such problems have been briefly addressed: (1) quantification of the accuracy of image (or superposition) methods for solving potential problems, and (2) resolution capabilities of prospecting methods based on d.c. electric conduction. We view the resolution phenomenon as an archetypal problem that can be examined via this potential solution. Crude resolution limits can be posed in terms of pickable extrema or inflection points on a voltage anomaly curve. More refined analysis would involve detailed measurements of the amplitude, width, and shape of the potential or apparent resistivity response as a selected parameter is varied. A quantitative appraisal of the resolving power of the technique, with or without the addition of measurement noise or positioning uncertainty, can thus be conducted. Finally, the capabilities of the potential solution for conducting forward modelling of mise à la masse and crosshole potential surveys has been demonstrated. Such versatility is naturally inherent in a general solution to the problem.

APPENDIX A: BISPHERICAL COORDINATES

The transformation from rectangular coordinates (x, y, z) to bispherical coordinates (μ, η, ϕ) is (Large 1971):

$$\mu(x, y, z) = \tfrac{1}{2} \ln \left[\frac{x^2 + y^2 + (z + b)^2}{x^2 + y^2 + (z - b)^2} \right], \qquad (-\infty < \mu < +\infty) \tag{A1}$$

$$\eta(x, y, z) = \tan^{-1} \left[\frac{2b\sqrt{x^2 + y^2}}{x^2 + y^2 + z^2 - b^2} \right], \qquad (0 \leq \eta \leq \pi) \tag{A2}$$

$$\phi(x, y, z) = \tan^{-1} \left[\frac{y}{x} \right]. \qquad (0 \leq \phi < 2\pi) \tag{A3}$$

The inverse transformation is (Grant and West 1965, p. 421):

$$x(\mu, \eta, \phi) = \frac{b \sin \eta \cos \phi}{\cosh \mu - \cos \eta}, \qquad (-\infty < x < +\infty) \tag{A4}$$

$$y(\mu, \eta, \phi) = \frac{b \sin \eta \sin \phi}{\cosh \mu - \cos \eta}, \qquad (-\infty < y < +\infty) \tag{A5}$$

$$z(\mu, \eta, \phi) = \frac{b \sinh \mu}{\cosh \mu - \cos \eta}. \qquad (-\infty < z < +\infty) \tag{A6}$$

From (A1), it is easy to demonstrate that a surface constant μ is a sphere with centre located on the z-axis at $(0, 0, b \coth \mu)$ and radius $b/|\sinh \mu|$. Hence, the bispherical coordinates μ_2 and μ_3 of the two spherical interfaces are:

$$\mu_2 = \sinh^{-1} (b/a_2) = \ln \left[\left(\frac{b}{a_2} \right) + \sqrt{\left(\frac{b}{a_2} \right)^2 + 1} \right], \tag{A7}$$

$$\mu_3 = -\sinh^{-1} (b/a_3) = -\ln \left[\left(\frac{b}{a_3} \right) + \sqrt{\left(\frac{b}{a_3} \right)^2 + 1} \right]. \tag{A8}$$

The scale factor b determines the location of the two poles of the bispherical coordinate system. We must have

$$d = b(\coth \mu_2 - \coth \mu_3),$$

$$b = a_2 \sinh \mu_2,$$

$$b = -a_3 \sinh \mu_3.$$

Solution of this system of equations for b yields

$$b = \frac{1}{2d} \{[d^2 - a_2^2 - a_3^2]^2 - 4a_2^2 a_3^2\}^{1/2}. \tag{A9}$$

APPENDIX B: SPHERICAL HARMONICS

A definition of the spherical harmonics and a description of their basic properties can be found in most textbooks on mathematical physics. Since there exist a variety of ways to define and normalize these functions, we explicitly state the forms utilized in the derivation here. Our formulae are taken mainly from Wyld (1976). The spherical harmonic of degree l and order m is defined as

$$Y_l^m(\theta, \phi) = \epsilon_m \sqrt{\frac{2l + 1}{2} \frac{(l - |m|)!}{(l + |m|)!}} \, P_l^{|m|}(\cos \theta) \frac{e^{+im\phi}}{\sqrt{2\pi}}, \tag{B1}$$

$l = 0, 1, 2, \ldots$ and $m = -l, -l + 1, \ldots, l - 1, l$. $\epsilon_m = (-1)^m$ for $m \geq 0$ and $\epsilon_m = 1$ for $m < 0$. $P_l^{|m|}(\cos \theta)$ is the associated Legendre polynomial of degree l and order m. Obviously, the zero-order harmonic is independent of the azimuthal angle ϕ.

The spherical harmonics are orthonormal in the following sense

$$\int_0^{2\pi} \int_0^\pi Y_l^m(\theta, \phi) Y_k^n(\theta, \phi)^* \sin \theta \, d\theta \, d\phi = \delta_{kl} \delta_{mn}. \tag{B2}$$

The choice of phase in (B1) implies that even/odd ordered spherical harmonics possess Hermitian symmetry/anti-symmetry:

$$Y_l^{-m}(\theta, \phi) = (-1)^m Y_l^m(\theta, \phi)^*. \tag{B3}$$

Suppose Θ is the angle between the two directions in space specified by the angular coordinates (θ_1, ϕ_1) and (θ_2, ϕ_2). The spherical harmonic addition theorem is an expansion of the Legendre polynomial $P_l(\cos \Theta)$ in terms of the spherical harmonics with arguments defining these two directions:

$$P_l(\cos \Theta) = \left(\frac{4\pi}{2l + 1}\right) \sum_{m=-l}^{+l} Y_l^m(\theta_1, \phi_1) Y_l^m(\theta_2, \phi_2)^*, \tag{B4}$$

with

$$\cos \Theta = \cos \theta_1 \cos \theta_2 + \sin \theta_1 \sin \theta_2 \cos (\phi_1 - \phi_2). \tag{B5}$$

The following 'sum and integral' property of the spherical harmonics is a generalization of the integral theorem for the associated Legendre polynomials stated by Large (1971):

$$\sum_{l=0}^\infty \sum_{m=-l}^{+l} q_{lm} \int_0^{2\pi} \int_0^\pi Y_l^m(\theta, \phi) Y_k^n(\theta, \phi)^* \sin \theta \cos \theta \, d\theta \, d\phi$$

$$= \frac{1}{2\sqrt{k + \frac{1}{2}}} \left\{ q_{k-1,n} \sqrt{\frac{k^2 - n^2}{k - \frac{1}{2}}} + q_{k+1,n} \sqrt{\frac{(k + 1)^2 - n^2}{k + \frac{3}{2}}} \right\}, \tag{B6}$$

where q_{lm} is any quantity that does not depend on θ or ϕ.

Finally, the generating function theorem for the Legendre polynomials is

$$[1 - 2ux + u^2]^{-1/2} = \sum_{l=0}^\infty u^l P_l(x), \qquad |u| < 1. \tag{B7}$$

APPENDIX C: FUNCTION DEFINITIONS

The functions appearing on the left-hand sides of (16a) and (16b) are defined as follows:

$$\alpha_{lm}(\mu) = (l + \tfrac{1}{2})^{1/2}((l + 1)^2 - m^2)^{1/2} e^{-(l+1/2)\mu}, \tag{C1}$$

$$\beta_l(\mu, \chi) = (l + \tfrac{1}{2})^{1/2}[\chi \sinh \mu - (2l + 1) \cosh \mu]e^{-(l+1/2)\mu}, \tag{C2}$$

$$\gamma_{lm}(\mu) = (l + \tfrac{1}{2})^{1/2}(l^2 - m^2)^{1/2} e^{-(l+1/2)\mu}. \tag{C3}$$

The function β is evaluated at two arguments given by

$$\chi_{12} = \frac{1 - \rho_1/\rho_2}{1 + \rho_1/\rho_2}, \qquad \chi_{13} = \frac{1 - \rho_1/\rho_3}{1 + \rho_1/\rho_3}.$$

The right-hand side function of (16a) and (16b) is

$$\delta_{lm}(\mu, v; \eta_s, \phi_s) = \frac{1}{l - \tfrac{1}{2}} \alpha_{l-1,m}(\mu + v)Y^m_{l-1}(\eta_s, \phi_s)^*$$

$$+ \frac{1}{l + \tfrac{1}{2}} \beta_l(\mu, 1)e^{-(l+1/2)v} Y^m_l(\eta_s, \phi_s)^*$$

$$+ \frac{1}{l + \tfrac{3}{2}} \gamma_{l+1,m}(\mu + v)Y^m_{l+1}(\eta_s, \phi_s)^*. \tag{C4}$$

Equations (16a) and (16b) are appropriate for a current electrode located in the unbounded medium. If the source is placed in the upper sphere ($\mu_s > \mu_2$) then the function on the right-hand side of (16a) is replaced by $-\delta_{lm}(-\mu_2, \mu_s; \eta_s, \phi_s)$. If the source is placed in the lower sphere ($\mu_s < \mu_3$) then the right-hand side function of (16b) is altered to $-\delta_{lm}(\mu_3, -\mu_s; \eta_s, \phi_s)$.

For the single sphere in a half-space problem, the coefficients in (25) are expressed in terms of previously defined functions:

$$a_{lm} = \left(\frac{\rho_1}{\rho_2} - 1\right)\alpha_{lm}(\mu_2) + \left(\frac{\rho_1}{\rho_2} + 1\right)\alpha_{lm}(-\mu_2), \tag{C5}$$

$$b_l = \left(\frac{\rho_1}{\rho_2} - 1\right)\beta_l(\mu_2, 1) + \left(\frac{\rho_1}{\rho_2} + 1\right)\beta_l(-\mu_2, \chi_{12}), \tag{C6}$$

$$c_{lm} = \left(\frac{\rho_1}{\rho_2} - 1\right)\gamma_{lm}(\mu_2) + \left(\frac{\rho_1}{\rho_2} + 1\right)\gamma_{lm}(-\mu_2). \tag{C7}$$

These coefficients can be reduced to forms similar to those of Large (1971) by substituting in the definitions of the functions α, β and γ. The correspondence is not exact however, because Large's equations contain some source position dependence on the left-hand side.

Where the current electrode is located outside the buried sphere, the right-hand side quantity d_{lm} in (25) is

$$d_{lm} = 2\pi\left(1 - \frac{\rho_1}{\rho_2}\right)[\delta_{lm}(\mu_2, \mu_s; \eta_s, \phi_s) + \delta_{lm}(\mu_2, -\mu_s; \eta_s, \phi_s)]. \qquad (C8)$$

If the current source is within the spherical conductor, then

$$d_{lm} = 2\pi\left(1 - \frac{\rho_1}{\rho_2}\right)[\delta_{lm}(\mu_2, \mu_s; \eta_s, \phi_s) - \delta_{lm}(-\mu_2, \mu_s; \eta_s, \phi_s)]. \qquad (C9)$$

Expressing the coefficients in the linear equations as such functions greatly facilitates programming of the solution on a computer. Values can be easily generated by utilizing FORTRAN FUNCTION subroutines.

REFERENCES

ELKINS, T.A. and HAMMER, S. 1938. The resolution of combined effects, with applications to gravitational and magnetic data. *Geophysics* **3**, 315–331.

GRANT, F.S. and WEST, G.F. 1965. *Interpretation Theory in Applied Geophysics.* McGraw-Hill Book Co.

KALLWEIT, R.S. and WOOD, L.C. 1982. The limits of resolution of zero-phase wavelets. *Geophysics* **47**, 1035–1046.

LARGE, D.B. 1971. Electric potential near a spherical body in a conducting half-space. *Geophysics* **36**, 763–767.

LIPSKAYA, N.V. 1949. The field of a point electrode observed on the earth's surface near a buried conducting sphere. *Doklady Akademii Nauk SSSR, Series Geografiya i Geofizika* **13**, 409–427.

MERKEL, R.H. and ALEXANDER, S.S. 1971. Resistivity analysis for models of a sphere in a halfspace with buried current sources. *Geophysical Prospecting* **19**, 640–651.

RICKER, N.H. 1953. Wavelet contraction, wavelet expansion, and the control of seismic resolution. *Geophysics* **18**, 769–792.

SNYDER, D.D. and MERKEL, R.H. 1973. Analytic models for the interpretation of electrical surveys using buried current electrodes. *Geophysics* **38**, 513–529.

TELFORD, W.M., GELDART, L.P., SHERIFF, R.E. and KEYS, D.A. 1976. *Applied Geophysics.* Cambridge University Press.

VAN NOSTRAND, R.G. 1953. Limitations on resistivity methods as inferred from the buried sphere problem. *Geophysics* **18**, 423–433.

WYLD, H.W. 1976. *Mathematical Methods for Physics.* W. A. Benjamin Inc.